Crustal trace of a hot convective sheet

Suleiman Al-Kindi*
Nicky White*
Bullard Laboratories, Madingley Rise, Madingley Road, Cambridge CB3 0EZ, UK
Martin Sinha* Southampton Oceanography Centre, University of Southampton, Waterfront Campus, European Way, Southampton SO14 3ZH, UK
Richard England* Department of Geology, University of Leicester, University Road, Leicester LE1 7RH, UK
Richard Tiley* Bullard Laboratories, Madingley Rise, Madingley Road, Cambridge CB3 0EZ, UK

ABSTRACT

The Iceland plume has played an influential role in the evolution of the North Atlantic Ocean and margins over the past 60 m.y. It is believed that this plume formed at the conjunction of a tetrad of hot, subvertical, convective sheets. The impingement of these hot sheets at the base of the lithospheric lid caused decompressional melting, generating substantial quantities of high-temperature magma that were injected into the cold overlying lid. Over the next 10 m.y., these sheets partly coalesced to form a crudely axisymmetric plume head. Here we analyze the lithospheric fingerprint of one of these hot convective sheets. By forward and inverse modeling of densely sampled wide-angle seismic data, in conjunction with gravity observations, we determined the three-dimensional shape of magmatic underplating trapped within the lithosphere. The injection of this melt into the lithosphere generated substantial permanent and minor transient uplift of Earth's surface. Predicted and measured amounts of consequent denudation and sedimentation agree within error. Temporal variations in the patterns of deposition and oceanic circulation adjacent to the convective sheet show its evolution through time and space. Our results suggest that this linear sheet has probably been directly and indirectly responsible for cyclical events over ~60 m.y. These events have 0.5–1 and 4–6 m.y. periodicities, the existence of which may help to elucidate the dynamic behavior of convective sheets during and after impingement. Thus, in particular circumstances, surficial geological processes yield an indirect record of mantle convection and melt-generation processes.

Keywords: plumes, underplating, denudation, convection, wide-angle seismology.

INTRODUCTION

Plumes are striking manifestations of convective patterns within the mantle and can develop when subvertical sheets intersect and coalesce (Houseman, 1990). However, our quantitative understanding of the detailed temporal and spatial evolution of mantle plumes on Earth is poor. The best data are from theoretical studies and numerical experiments that show that mantle convection at high Rayleigh numbers with temperature-dependent viscosity is strongly time dependent (Schubert et al., 2001). Although predictions are made on the basis of these numerical experiments, we have few observational data for the spatial and temporal evolution of these convective sheets or for their evolution into bona fide axisymmetrical structures.

The intersection of a hot convective sheet with the lithosphere can affect Earth's surface in two related ways. First, transient uplift and subsidence are governed by the internal temperature structure and flow regime of the hot convective sheet. Such motions vary with time and directly reflect the dynamic evolution of the sheet. Second, permanent uplift and to some extent transient subsidence occur when liquid rock is generated by high-temperature melting above the sheet and injected into the lithosphere (Cox, 1993; Maclennan and Lovell, 2002). Here we use geophysical and geological data sets to define the history of vertical motions generated by one of the best candidates for the manifestation of a convective sheet (Fig. 1).

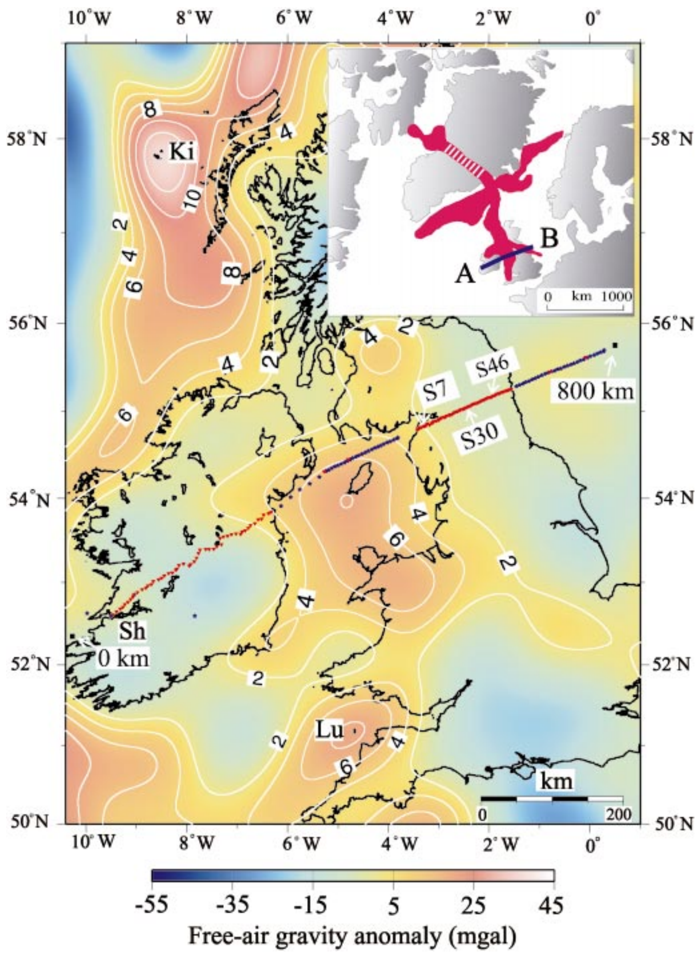

Figure 1. Long-wavelength, free-air gravity map showing positive anomaly centered on Irish Sea. Numbered white contours—predicted thickness of magmatic underplating determined by calibrating long-wavelength gravity data with wide-angle seismic model (see text for details). Red triangles—locations of 111 onshore and 4 offshore seismometers across England and Ireland; blue triangles—locations of 64 offshore and 2 onshore explosive shots for British and Irish Caledonian Suture Seismic Project (CSSP, ICSSP) wide-angle seismic experiments, which traverse 800 km (29 smaller shots and 1 large one in North Sea and 25 in Irish Sea). S7, S30, and S46 are seismometer stations referred to in text and in Figure 2. Sh—Shannon River estuary; Lu—Lundy; Ki—St. Kilda. Inset: Reconstruction of North Atlantic region at initiation of Iceland plume just before continental breakup. Solid red pattern—onshore-offshore distribution of magmatism, which is crustal manifestation of intersecting convective sheets; solid blue line AB—CSSP, ICSSP seismic experiment.

*E-mail addresses: Al-Kindi—kindi@esc.cam.ac.uk; Tiley—tiley@esc.cam.ac.uk; Sinha—sinha@soc.soton.ac.uk; England—rwe5@le.ac.uk. Corresponding author: White—nwhite@esc.cam.ac.uk.

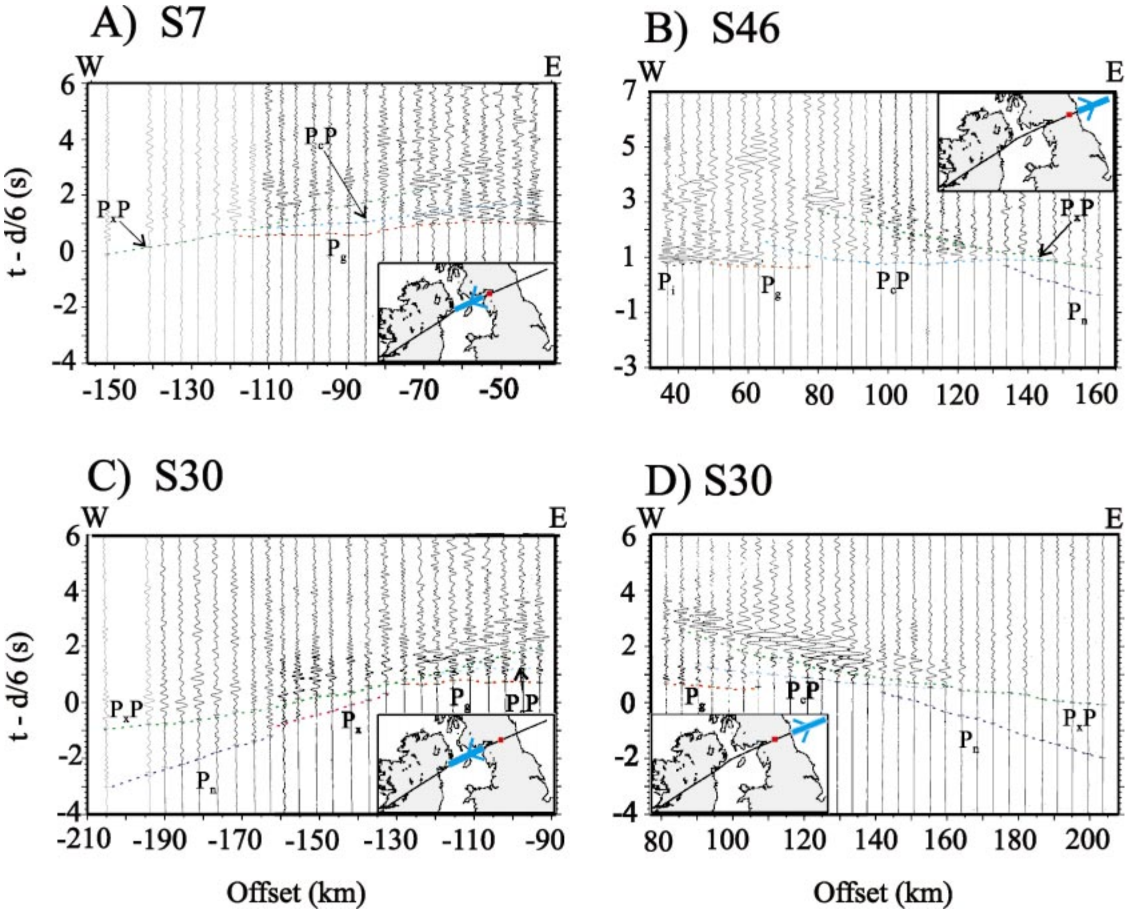

Figure 2. Wide-angle seismograms from three stations located onshore England. Traveltimes are reduced at 6 km s^{-1} (i.e., horizontal arrivals travel at 6 km s^{-1} hence *t* – *d*/6). Colored dashed lines highlight picks used in modeling. Black P_i and red P_g phases—upper crustal diving waves traveling at velocities of <~6 km s^{-1}; light blue P_cP phase—mid-crustal reflections; magenta P_x phase—lower crustal diving waves travelling at velocity of ~7.5 km s^{-1}; green P_xP phases—lower crustal reflections; dark blue P_n phase—upper mantle diving wave traveling at velocity of ~8 km s^{-1}. In each case, red circle and blue arrow show location of each station-shot pair and direction in which energy travels, respectively. A: Seismometer S7, close to west coast of England, recorded Irish Sea shots. B: S46, close to east coast of England, recorded North Sea shots. C: S30, in center of England, recorded Irish Sea shots. Note that slopes of P_x and P_n are similar but not identical. D: S30 recorded North Sea shots.

During the initiation and early stages of the Iceland plume, a tetrad of intersecting sheets developed (Barton and White, 1997). The most obvious manifestation of these sheets is the copious amount of synchronous, high-temperature intrusive and extrusive magmatism (Fig. 1; Cox, 1993; White and McKenzie, 1989). One pair of sheets was oriented parallel to the incipient rift that later formed the North Atlantic Ocean between Greenland and Europe. A second pair developed at right angles, and extended from Disko Island off the west coast of Greenland to Lundy in southern Britain. We are primarily interested in the sheet beneath the British Isles, because its surficial expression can be measured in many different ways. Furthermore, the history of vertical motions of this sheet has not been overprinted by coeval rifting and subsidence, unlike the orthogonal set of sheets that parallels the rifted margins and whose actual existence is more controversial.

SEISMIC EXPERIMENT

Design

We first map the magmatic fingerprint of the convective sheet within the lithosphere, then investigate the link between deep structure and surface expression with a view to determining the temporal history of this sheet. Dense wide-angle seismic observations delimit crustal structure at right angles to the putative convective sheet (Fig. 1). The wide-angle experiment was designed and implemented as part of the British and Irish Caledonian Suture Seismic Project (CSSP and ICSSP) by Bott et al. (1985) and Jacob et al. (1984). Although preliminary and separate interpretations of parts of CSSP and ICSSP were made (Bott et al., 1985; Jacob et al., 1984; Lewis, 1986), there is no integrated and consistent model based on all seismograms. Past interpretation was hampered by the absence of near-surface velocity control. In our combined modeling of these data, we used modern well logs and shallow seismic reflection lines to define near-surface velocity associated with deep sedimentary basins. We also used two-dimensional forward and inverse modeling algorithms, which were unavailable when this ambitious experiment was executed.

The combined seismic line starts in the North Sea, crosses the British Isles, and culminates in the Shannon River estuary (Fig. 1). A total of 64 explosive shots was detonated close to the seabed at ~4 km shot spacing in the North Sea, in the Irish Sea, and in the Shannon estuary. The majority of shots consisted of 150 kg of Imperial Chemical Industries (ICI) Geophex; several 450 kg shots and quarry blasts were also detonated. These shots were recorded across northern England by 60 three-component seismometers, which were deployed at 2 km spacing (Fig. 1). In Ireland, 51 seismometers were deployed at 5 km intervals from the Irish Sea to the Shannon estuary. The seismic data are of high quality: a typical set of shot gathers is shown in Figure 2. Records clearly have excellent signal-to-noise ratios and are dominated by wide-angle (i.e., postcritical) reflections with large amplitudes and by refractions with smaller amplitudes.

Forward Modeling

Six dominant wide-angle phases have been identified, and more than 2900 traveltime picks were analyzed using RAYINVR, a ray-based forward-modeling package developed by Zelt and Smith (1992) (Figs. 2, 3A, 3B). First, we carefully modeled the P_i and P_g phases, which are short- and medium-offset arrivals generated by energy refracting within the uppermost crust. We corroborated this upper crustal

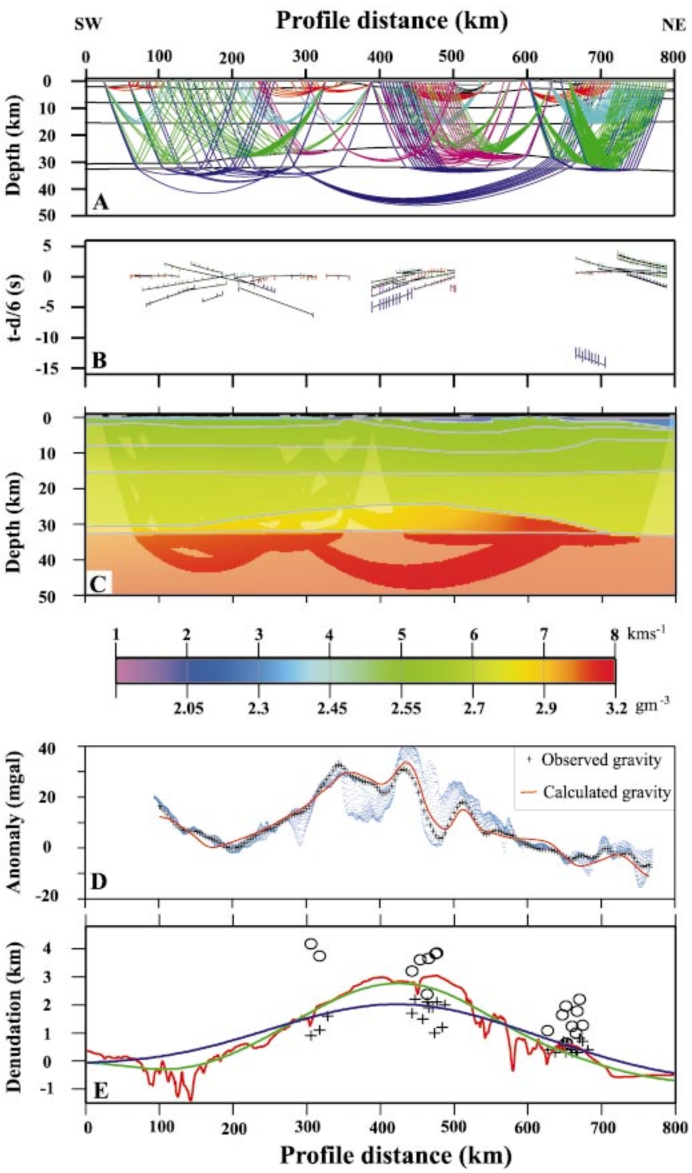

Figure 3. A: Subset of 371 P wave rays that define velocity structure of crust and upper mantle using color scheme shown in Figure 2 (total of 2943 rays define model). B: Traveltime picks reduced at 6 km s^{-1} (hence *t* − *d*/6). Colored vertical bars—observed picks of different phases; length of bar—three times actual degree of uncertainty; black lines—predicted picks based on forward modeling through velocity structure using RAYINVR algorithm of Zelt and Smith (1992). C: Optimal velocity structure of crust and upper mantle determined by iterative forward modeling. This model is smoothest that also satisfied least squared misfit criteria. Greater color intensity highlights ray coverage, delineating areas where model is best defined. Very similar solution was obtained by automated inverse modeling (JIVE algorithm of Hobro et al., 2003). Lower set of numbers on color scale—velocity values; upper set of numbers—density values calculated from velocities using empirical relationship of Christensen and Mooney (1995). Lithostatic pressure along base of our density model varies by <1%. D: Gravity model calculated from wide-angle model. Black crosses—observed free-air gravity anomaly; envelope of blue points—observed gravity anomalies in corridor of ±10 km each side of line; red line—predicted gravity anomaly using density model shown in C. E: Black crosses—denudation of rock (i.e., erosion) at Earth's surface calculated by inverse modeling of subsidence data; circles—denudation calculated by inverse modeling of vitrinite reflectance data. Red line—denudation predicted using crustal model shown in C and assuming Airy isostasy (i.e., elastic thickness = 0 km); green and blue lines—denudation for elastic thicknesses of 20 and 50 km, respectively.

model using independent observations from surface geology, well logs, and shallow seismic surveys. Once the misfit between observed and predicted traveltime picks was minimized according to least squares criteria, the velocity structure of the lower crust and upper mantle was calculated. The most important phases for defining deeper structure are large-amplitude, wide-angle reflected arrivals, P_xP, and weak upper mantle refracted arrivals, P_n. It is impossible to fit both phases simultaneously using a simple crustal structure. Instead, these data require the existence of a high-velocity welt within the lower crust. Careful inspection of shot records shows that the P_n phase can be subdivided into P_x, whose rays turn within the welt, and P_n sensu stricto. P_xP is a wide-angle reflection from the top of the high-velocity welt and there is also evidence for reflections from its base (i.e. P_mP sensu stricto; see Fig. 2C at ranges of −130 to −90 km and at reduced traveltimes of ~0.5 s behind P_xP).

A smooth forward model, which satisfies least squares criteria, is shown in Figure 3B. Ray coverage is good except in the middle of the profile, between 350 and 450 km. The best-defined part of the model is from 400 to 800 km, where station coverage was dense and where the signal-to-noise ratio was excellent. At 550 km, the line intersects another wide-angle profile, where both crustal models agree to within several kilometers (Barton, 1992). The velocity of the welt varies from 7.2 to 7.6 km/s and has a maximum thickness of 8 ± 1 km beneath the Isle of Man. Its upper and lower surfaces have been determined to within ±0.3 and ±1.3 km, respectively. Toward the northeast, this high-velocity welt pinches out at a distance of 700 ± 20 km. There is insufficient ray coverage at the southwest end, where the welt may die out. Resolution kernels were calculated for representative velocity and depth nodes, showing that the model is well resolved and not overparameterized. We have independently checked our crustal model by inverting the traveltime picks using JIVE, an iterative tomographic traveltime inversion algorithm developed by Hobro et al. (2003). A simple one-dimensional starting model, which consists of a uniform crustal structure with no lower crustal welt, was used and ~25 iterations were required to achieve a misfit of $\chi^2 \sim 1$. The inverted solution closely resembles that in Figure 3C having average differences of ±0.2 km/s. Gravity modeling provides another important check. Using Christensen and Mooney's (1995) empirical relationship between seismic velocity and density, we calculated the free-air gravity anomaly along the seismic line. Predicted and measured gravity anomalies are in excellent agreement (Fig. 3D). We have used this agreement to design a simple wavelength-dependent function that calculates the shape of the welt from the gravity anomaly in three dimensions (the long-wavelength gravity anomaly was first calculated using a low-pass filter of 150 km with a suitable taper and then multiplied by ~0.27 km/mgal: Fig. 1; Wessel and Smith, 1995). The resultant three-dimensional distribution of magmatic underplating is complex. We acknowledge that this extrapolation must be treated with caution away from the wide-angle line because there could be other geological explanations for the observed gravity anomalies. Nevertheless, our extrapolation is corroborated in several places both by legacy and by unpublished wide-angle lines. In the northwest corner of Figure 1, free-air gravity edge effects mean that the predicted thickness of underplate may be overestimated by about one-half.

Geological Implications

The composition and age of this three-dimensional body are defined by a range of self-consistent geological and geophysical observations. We note that there may be other geological interpretations for this body, but we believe that our explanation is the most likely one because it is supported by a range of disparate observations. First, the welt's high velocity and density are consistent with those of a cumulate mafic igneous rock (e.g., gabbro) that crystallized from a liquid generated by melting of a mantle source with a potential temperature of ≥1500 °C, in broad agreement with geochemical calculations (Maclennan and Lovell, 2002). Prominent P_xP phases are accompanied by high-amplitude coda (Fig. 2). One- and two-dimensional reflectivity modeling, using the methods of Fuchs and Muller (1971) and Zelt and Smith (1992), shows that the amplitude and duration of these coda can be accounted for by kilometer-scale internal layering. This layering could conceivably have been generated following a single injection of melt, but it is more likely that it was generated by multiple injections. Second, the spatial distribution of magmatic underplating broadly coincides with the loci of major Paleogene igneous centers. At the northern end, a calculated underplate of ~12 km coincides with the island of St. Kilda, which is an important igneous complex. At the southern end, the calculated underplate coincides with the Lundy complex (Fig. 1). Within the Irish Sea, there is excellent evidence for widespread dike intrusion. Third, emplacement of magmatic underplating will generate substantial uplift and denudation (Cox, 1993; White and Lovell, 1997). In Figure 3E, the shape and density of the magmatic welt were used to calculate the amplitude and wavelength of permanent denudation for a range of lithospheric elastic thicknesses. The locus, amount, and inferred timing of predicted and measured denudation are in close agreement. Nonetheless, our denudation measurements have scatter and cannot preclude the modulating effect of intermittent phases of transient uplift for which there is independent evidence (Jones et al., 2002).

This denudation triggered a flux of clastic sediments into the surrounding offshore basins between 61 and 54 Ma (White and Lovell, 1997). The period of sedimentation agrees well with the duration of magmatism and shows that the convective sheet was generating melt over a period of time. Temporal variations in clastic deposition and magmatism together with evidence for internal layering of the magmatic underplate suggest that melt was generated and injected with a periodicity of ~1 m.y. This periodicity is corroborated by the existence of transgressive mud sequences, which can be explained by episodes of melt solidification (Maclennan and Lovell, 2002).

DISCUSSION

By combining our results with evidence for phases of regional uplift and denudation, we can begin to outline the temporal behavior of the inferred hot convective sheet over a 60 m.y. period. The offshore sedimentary record suggests that this sheet impinged upon the base of the lithosphere at least ~2 m.y. before decompression melting began ca. 61 Ma. This melting was not caused by passive rifting, for which there is no evidence at this time. Approximately synchronous phases of clastic sedimentation with periodicities of 0.5–1 m.y. accompanied magmatic underplating. The phase of greatest sedimentation coincided with the acme of magmatism at 59 Ma. These relationships strongly suggest that melt generation and/or emplacement varied on time scales of 0.5–1 m.y. Internal layering of the magmatic underplate supports this suggestion. The cross-sectional and planformal shape of this underplate is surprisingly complex and has important implications for our understanding of melt injection (Fig. 1). At 54 Ma, magmatism ceased and the volume of clastic sedimentation abruptly declined by several orders of magnitude. We infer that the temperature within the convective sheet decreased and the subsequent period of relative quiescence lasted until 35 Ma. From that time until the present day, hundreds of meters of uplift and subsidence with periodicities of 5–6 m.y. and 2–3 m.y. occurred along the Iceland-Faroe-Scotland Ridge (Wright and Miller, 1996; Jones et al., 2002). Since the Miocene (i.e., ca. 17 Ma), production of North Atlantic Deep Water and of its precursor, Northern Component Water, has been strongly modulated by variations in the height of this ridge. Thus, although the Iceland plume is regarded as an approximately axisymmetric structure, it is possible that the remnants of at least one of the original hot convective sheets may continue to exist, albeit at lower temperatures. The presence of such a sheet is manifest by a linear long-wavelength gravity anomaly over the British Isles.

In summary, dense wide-angle seismic data in conjunction with a large body of geological and geophysical observations permit us to extract detailed information about the Cenozoic history of a hot convective sheet that forms part of the Iceland plume structure. The spatial and temporal interactions between this sheet and the overlying lithosphere will help us to understand the details of convective dynamics.

ACKNOWLEDGMENTS

Al-Kindi was supported by Petroleum Development Oman. We are grateful to P. Barton, R. Edwards, R. Hobbs, J. Hobro, S. Jones, B. Lovell, D. Lyness, S. Singh, and R. White for their help. Figures were prepared using Generic Mapping Tools of Wessel and Smith (1995). University of Cambridge, Department of Earth Sciences Contribution 7212.

REFERENCES CITED

Barton, A.J., and White, R.S., 1997, Crustal structure of the Edoras Bank continental margin and mantle thermal anomalies beneath the North Atlantic: Journal of Geophysical Research, v. 102, p. 3109–3129.

Barton, P., 1992, LISPB revisited: A new look under the Caledonides of northern Britain: Geophysical Journal International, v. 110, p. 371–391.

Bott, M.H.P., Long, R.E., Green, A.S.P., Lewis, A.H.J., Sinha, M.C., and Stevenson, D.L., 1985, Crustal structure south of the Iapetus suture beneath northern England: Nature, v. 314, p. 724–727.

Christensen, N.I., and Mooney, W.D., 1995, Seismic velocity structure and composition of the continental crust: A global view: Journal of Geophysical Research, v. 100, p. 9761–9788.

Cox, K.G., 1993, Continental magmatic underplating: Royal Society of London Philosophical Transactions, ser. A, v. 342, p. 155–166.

Fuchs, K., and Muller, G., 1971, Computation of synthetic seismograms with the reflectivity method and comparison with observation: Royal Astronomical Society Geophysical Journal, v. 23, p. 417–433.

Hobro, J., Singh, S., and Minshull, T., 2003, Three-dimensional tomographic inversion of reflection and wide-angle datasets: Geophysical Journal International (in press).

Houseman, G.A., 1990, The thermal structure of mantle plumes: Axisymmetric or triple junction?: Geophysical Journal International, v. 102, p. 15–24.

Jacob, A.W.B., Kaminski, W., Murphy, T., Phillips, W.E.A., and Prodehl, C., 1984, A crustal model for a northeast-southwest profile through Ireland: Tectonophysics, v. 113, p. 75–103.

Jones, S.M., White, N., and Maclennan, J., 2002, V-shaped ridges around Iceland: Implications for spatial and temporal patterns of mantle convection: Geochemistry Geophysics Geosystems v. 3, no. 10, 1059 (DOI 10.1029/2002 GC 000361).

Lewis, A.H.J., 1986, The deep seismic structure of northern England and adjacent marine areas from the Caledonian Suture Seismic Project [Ph.D. thesis]: Durham, UK, University of Durham, 641 p.

Maclennan, J., and Lovell, B., 2002, Control of regional sea level by surface uplift and subsidence caused by magmatic underplating of Earth's crust: Geology, v. 30, p. 675–678.

Schubert, G., Turcotte, D.L., and Olson, P., 2001, Mantle convection in the Earth and planets: Cambridge, Cambridge University Press, 940 p.

Wessel, P., and Smith, W.H.F., 1995, New version of the generic mapping tools released: Eos (Transactions, American Geophysical Union), v. 76, p. 329.

White, N., and Lovell, B., 1997, Measuring the pulse of a plume with the sedimentary record: Nature, v. 387, p. 888–891.

White, R.S., and McKenzie, D., 1989, Magmatism at rift zones: The generation of volcanic continental margins and flood basalts: Journal of Geophysical Research, v. 94, p. 7685–7730.

Wright, J.D., and Miller, K.G., 1996, Control of North Atlantic Deep Water circulation by the Greenland-Scotland Ridge: Paleoceanography, v. 11, p. 157–170.

Zelt, C.A., and Smith, R.B., 1992, Practical and efficient ray tracing in two-dimensional media for rapid travel time and amplitude forward modelling: Geophysical Journal International, v. 108, p. 16–34.

Manuscript received 11 July 2002
Revised manuscript received 23 October 2002
Manuscript accepted 2 November 2002

Printed in USA